

Defect-deformation mechanism of spontaneous nucleation of an ensemble of pores in solids and its experimental verification

V.I. Emel'yanov, K.I. Eremin, V.V. Starkov

Abstract. The defect-deformation (DD) mechanism of spontaneous formation of ensembles of seed pores during etching of semiconductors and metals is developed. The mechanism is based on the concept of generation and DD self-organisation of interstices and vacancies during etching. For p-Si, good agreement between theoretical and experimental results is obtained. In particular, a quasi-hexagonal order in the arrangement of micropores on the surface is revealed, which was predicted by the DD model, and a control of the properties of the ensemble by means of external forces is demonstrated.

Keywords: micropores, surface etching, self-organisation.

1. Interest in the physics of formation of ensembles of micropores in semiconductors and metals upon electrochemical etching is explained by applications of microporous Si, in particular, in a new laser technology involving photonic crystals [1, 2]. However, the physical mechanism of spontaneous formation of ensembles of micropores is not conclusively established so far. Indeed, similar systems of micropores are formed both in semiconductors and metals, for example, in Al [3], whereas the hole models of their formation are valid only for semiconductors [4, 5]. Note also that the spatial distribution of pores on a surface was considered random up to now.

2. In this paper, we develop a universal defect-deformation (DD) mechanism of spontaneous formation of a seed ensemble of pores on the surface of semiconductors and metals, which consists in the following. Consider the surface of a solid $z = 0$ (the z axis is directed into the medium) in contact with an etching agent. During an elementary etching event, a surface atom (ion) located in the crystal lattice of the solid loses its bonds with neighbouring atoms and passes either to the etching agent [with the probability γ_e (s^{-1})] or to a near-surface interatomic plane with the formation of an interstice [with the probability γ_i (s^{-1})]. This is accompanied by the appearance of a vacancy, which can be considered

remaining at the interface $z = 0$ because of its low mobility. Then, mobile intrinsic interstices diffuse deep in a sample, thus forming a near-surface layer enriched with interstices if the diffusion rate is higher than the rate V of spatially homogeneous etching: $D_i/a > V = (\gamma_e + \gamma_i)a$, where a is the sample lattice constant and D_i is the diffusion coefficient of an interstice.

The dependence $n_i = n_i(z)$ of the concentration of interstices in the coordinate system moving with the surface $z = 0$ can be found from the equation $\partial n_i / \partial t - V \partial n_i / \partial z = D_i \partial^2 n_i / \partial z^2$ with the boundary condition $-D_i (\partial n_i / \partial z)_{z=0} = \gamma_i / a^2$, whose stationary solution gives $n_i(z) = a^{-3} [\gamma_i / (\gamma_i + \gamma_e)] \exp(-Vz/D_i)$.

3. An interstice-enriched near-surface layer can be treated as a 'film' with the effective thickness h (see below), which is rigidly connected with a part of a crystal ('substrate') located below. As shown earlier (see reviews [6, 7]), in such a film the DD instability develops when the interstice concentration exceeds the critical value $n_{cr} \sim 10^{19} \text{ cm}^{-3}$. This results in the formation of a stationary relief modulation grating $\zeta(\mathbf{r}) = A \exp[i\mathbf{q}\mathbf{r}] + \text{c.c.}$, where $\zeta(\mathbf{r})$ is a local displacement of the surface along the z axis ($\zeta > 0$ corresponds to the relief hollow), A is the amplitude, and \mathbf{q} is the grating vector; the interstices with the dilatation potential $\theta_i > 0$ being piled up in the relief protrusions ($\zeta < 0$). The surface vacancies generated during etching are collected in the relief hollows ($\theta_v < 0$), by producing a surface grating n_v of the vacancy concentration, which is in phase with the relief grating: $n_v(\mathbf{r}) = A|\beta| \exp[i\mathbf{q}\mathbf{r}] + \text{c.c.}$, where $|\beta| > 0$ [6, 7].

The effective thickness h of the interstice-enriched film is determined from the condition $n_i(h) = n_{cr}$. This yields $h = (D_i/V) \ln[a^{-3} \gamma_i / n_{cr}(\gamma_i + \gamma_e)]$. The period $\Lambda = 2\pi/q$ of the surface interstitial and, hence, vacancy grating is proportional to the 'film' thickness h and depends on the spatially homogeneous interstice concentration n_{i0} : $\Lambda = hf(n_{i0})$. For sufficiently large n_{i0} , the period is independent of the interstice concentration and is equal to $2h$ [6, 7].

A nonlinear computer analysis [8] of the film DD model [6] showed that a hexagonal periodic DD structure is formed on the isotropic surface due to the DD instability. Such a structure can be treated as a superposition of three DD gratings with the period $\Lambda = 2h$ and vectors \mathbf{q} , which form an equilateral triangle on the surface. Therefore, a cellular hexagonal distribution of the vacancy (seed pore) concentration with the characteristic period

$$\Lambda = \frac{2D_i}{V} \ln \left[\frac{a^{-3} \gamma_i}{n_{cr}(\gamma_i + \gamma_e)} \right] \quad (1)$$

V.I. Emel'yanov, K.I. Eremin Department of Physics, M.V. Lomonosov Moscow State University, Vorob'evy gory, 119899 Moscow, Russia;
V.V. Starkov Institute of Problems of Microelectronic Technology, Russian Academy of Sciences, 142432 Chernogolovka, Moscow oblast, Russia

Received 29 March 2002

Kvantovaya Elektronika 32 (6) 473–475 (2002)

Translated by M.N. Sapozhnikov

is formed on the surface moving at the velocity V due to the DD self-organisation.

4. The first, spatially homogeneous etching stage occurring at the rate V ends after the appearance of the surface hexagonal cellular structure of seed pores with the characteristic scale (1) and of the anti-phase hexagonal cellular interstice structure. Then, the regime of spatially inhomogeneous etching begins because, due to a local increase in the current density near the bottom of pores, the etching rate V_p of the pore bottom increases according to [5], so that $V_p \gg V$ and $V_p \gg V_i$ (where V_i is the etching rate of regions with interstice aggregations). Therefore, etching occurs only in the regions where seed pores are located, which should result in the formation of the hexagonal structure of the developed pores with the characteristic distance between their centres determined by expression (1).

5. To verify the predictions of the DD mechanism of formation of an ensemble of pores, we etched p -Si samples with the surface area $S = 6 \text{ cm}^2$ in a standard electrochemical cell. The (100) surface of samples was disoriented by 0.5° . The (100) Si samples with the resistance above $10^3 \Omega \text{ cm}$, as well as 23, 10, and $6 \Omega \text{ cm}$ were etched at the constant current density $J = 5.5 \text{ mA cm}^{-2}$ at room temperature in the $\text{HF} : \text{DMF} = 1 : 10$ or $\text{HF} : \text{H}_2\text{O} : (\text{CH}_3)_2\text{CHOH} = 5 : 9 : 26$ solution for 60 min. The SEM photographs of sample surfaces after etching (Fig. 1a) demonstrate the presence of an ensemble of pores, whose number density N_p increases monotonically with decreasing sample resistance (i.e., with increasing concentration n_a of the boron impurity). The experimental dependence of the number density $N_{p\text{exp}}$ of pores on n_a is shown in Fig. 2 together with the theoretical dependence

$$N_p = A^{-2} = N_{p0}(1 + Bn_a^{2/3})^2,$$

predicted by the DD mechanism, where $N_{p0} = A_0^{-2} \approx 5.9 \times 10^5 \text{ cm}^{-2}$ is the number density of pores on the pure crystal surface; $A_0 = (2D_i/V_0) \ln[a^{-3}\gamma_i/n_{cr}(\gamma_i + \gamma_e)]$ is the characteristic scale of pores in a pure crystal; $B = V_a\alpha/V_0a^{-2} = 8 \times 10^{10} \text{ cm}^2$ is a fitting parameter; V_a is the etching rate of a region around the implant impurity (it is assumed that $V_a \gg V_0$); $\alpha > 1$ is a dimensionless coefficient characterising the size of the region of accelerated etching around an impurity; and V_0 is the rate of spatially homogeneous etching of a pure crystal (for $a^{-3} = 5 \times 10^{22} \text{ cm}^{-3}$, $\alpha \sim 10$, and $V_a/V_0 \sim 10^5$).

To verify the prediction of the long-range hexagonal order in the arrangement of pores on the surface, we performed the two-dimensional computer Fourier transform of the SEM image of the sample surface after etching (Fig. 1a). The smoothed out amplitude part $|F(k_x, k_y)|$ of the Fourier spectrum is shown in Fig. 1b.

The most interesting feature of the spectrum is the presence of pairs of maxima, the maxima in each pair being located symmetrically with respect to the ring centre on the lines passing through its centre. The pairs form three groups. Each pair of maxima lying on the same diameter corresponds to the grating of the local surface image brightness, i.e., to the pore grating. Thus, the image in Fig. 1a is formed by three groups of pore gratings with the wave vectors \mathbf{q} having close moduli, which are directed at certain (different from 60°) angles to each other.

The ideal hexagonal order is violated in the case under study (Fig. 1) for the following reasons. The disorientation

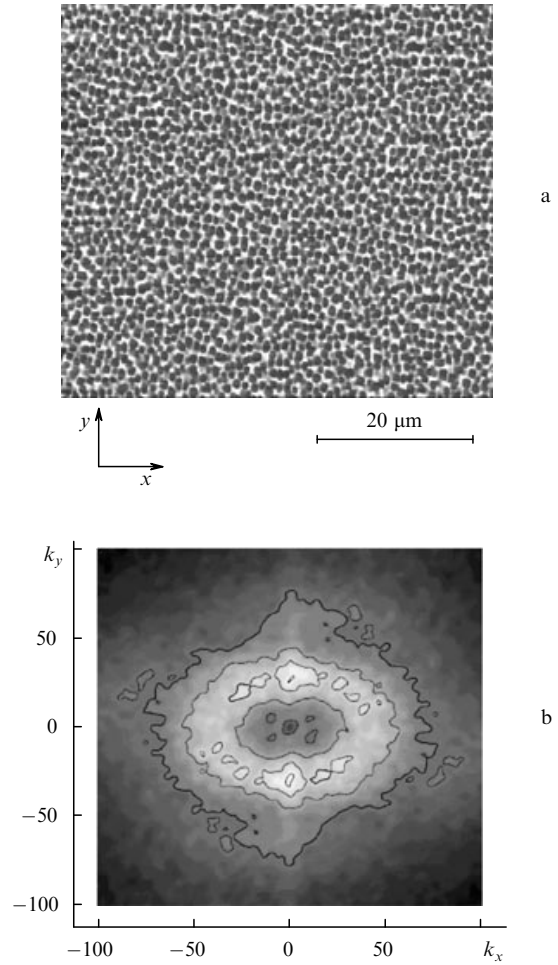


Figure 1. SEM image of the disoriented Si (100) surface (the disorientation angle is 0.5°) with the resistance $6 \Omega \text{ cm}$ after etching (a) and the smoothed out amplitude part $|F(k_x, k_y)|$ of the Fourier spectrum of the SEM image in Fig. 1a (b). Here, k_x and k_y are the reduced dimensionless wave numbers; the actual wave numbers are $q_x = 2\pi k_x/L_x$ and $q_y = 2\pi k_y/L_y$, where $L_x = 57.2 \mu\text{m}$ and $L_y = 51.2 \mu\text{m}$ are the sizes of the photographed part of the surface. Brighter regions correspond to larger values of $|F(k_x, k_y)|$. For samples with other resistances, the Fourier spectrum is similar.

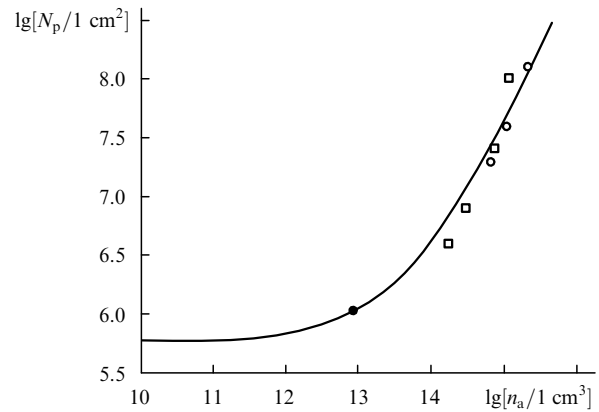


Figure 2. Dependence of the surface number density of pores on the volume concentration of the implant impurity obtained for the $\text{HF} - \text{DMF}$ (\circ) and $\text{HF} - \text{H}_2\text{O} - (\text{CH}_3)_2\text{CHOH}$ (\bullet) solutions, as well as obtained in [5] (\square). The solid curve corresponds to the theory.

of the Si surface induces the surface stress [stretch (or compression) along the y axis and compression (stretch) along the x axis in Fig. 1]. This is manifested in the Fourier spectrum (Fig. 1b) in the form of two symmetric protuberances of the rhombic plateau elongated along the y axis and two symmetric hollows ('negative' protuberances) directed along the x axis. The stretching (compression) uniaxial stress 'captures' one of the DD gratings by orienting its vector along the stretch (compression) direction [6, 7] and making it more intense. A pair of the most intense maxima in Fig. 1b corresponds to this stress-selected DD grating. On the contrary, the compressing (stretching) stress along the x axis results in the 'repulsion' of the vectors of DD gratings from the x axis direction. In addition, as follows from a computer analysis, three DD gratings have random phases, which also distorts the long-range hexagonal order in the pore distribution.

Note in conclusion that the DD mechanism can be generalised to the case of etching of meso- and nanopores. The results obtained in this paper open up the principal possibility of producing coherent (periodic) hexagonal ensembles of pores upon their spontaneous nucleation.

References

1. Chelnokov A., Wang K., Rowson S., et al. *Appl. Phys. Lett.*, **77**, 2943 (2000).
2. Miller F., Birner A., Cosele U., et al. *J. Porous. Mater.*, **7**, 201 (2000).
3. Li A.P., Muller F., Birner A., et al. *Adv. Mater.*, **11**, 483 (1999).
4. Valance A. *Phys. Rev. B*, **52**, 8323 (1995); *ibid*, **55**, 9706 (1997).
5. Lehmann V., Ronnebeck S. *J. Electrochem. Soc.*, **146**, 2968 (1999).
6. Emel'yanov V.I. *Laser Phys.*, **2**, 389 (1992).
7. Emel'yanov V.I. *Kvantovaya Elektron.*, **29**, 1 (1999) [*Quantum Electron.*, **29**, 839 (1999)].
8. Walgraef D., Ghoniem N.M., Lauzeral J. *Phys. Rev. B*, **56**, 15361 (1997).